

Submitted to the
XXII International Symposium on Lepton-Photon Interactions at High
Energy
30 June - 5 July 2005, Uppsala, Sweden

Abstract: 269

Sessions: QCD/HS, FP

Measurement of beauty production from dimuon events at HERA

ZEUS Collaboration

Abstract

Beauty production with events in which two muons are observed in the final state has been measured with the ZEUS detector at HERA using an integrated luminosity of 121 pb^{-1} . A low p_T threshold for muon identification, in combination with the large rapidity coverage of the ZEUS muon system, gives access to essentially the full phase space for beauty production. The dimuon selection suppresses backgrounds from charm and light flavour production. Separation of the sample into high- and low-mass, isolated and non-isolated, like- and unlike-sign muon pairs offers redundancy which is used to further constrain the backgrounds. The total cross section for beauty production at HERA, as well as differential cross sections and a measurement of $b\bar{b}$ correlations are obtained, and compared to QCD predictions.

1 Introduction

This paper reports measurements of beauty production via the reaction $ep \rightarrow b\bar{b}X \rightarrow \mu\mu X'$ using the ZEUS detector at HERA. The dimuon final state yields a data sample enriched in $b\bar{b}$ pairs, and with strongly suppressed backgrounds from other processes. This allows low p_T^μ -threshold cuts to be applied.

Conceptually, the analysis is very similar to the analysis of $D^* + \mu$ final states [1,2] with three significant differences. The larger branching ratio yields more statistics. The wider rapidity coverage allows the extraction of the total beauty production cross section with almost no extrapolation. The low charm background allows significant measurements of $b\bar{b}$ correlations.

In addition, this analysis complements measurements of beauty production based on single leptons with high transverse momentum [3,4], or on inclusive impact parameter tags [5,6].

2 Principle of the measurement

Two different event classes contribute to the beauty signal to be measured. First, events in which the two muons originate from the same parent b hadron, e.g. through the sequential decay chain $b \rightarrow c\mu X \rightarrow s\mu\mu X'$. These yield unlike-sign dimuon pairs produced in the same hemisphere and constrained to dimuon invariant masses of $m_{\text{inv}}^{\mu\mu} < 4$ GeV (i.e. a partially reconstructed B -meson mass). Secondly, events in which the two muons originate from different beauty quarks of a $b\bar{b}$ pair. These can yield both like- and unlike-sign dimuon combinations, depending on whether the muon originates from the decay of the primary beauty quark, or from a secondary charm quark, and whether $B^0 - \bar{B}^0$ mixing has occurred. Such muons will predominantly be produced in different hemispheres, and tend to have a large dimuon mass.

An important background contribution arises from charm-pair production, where both charm quarks decay into a muon. This yields unlike-sign dimuon pairs only, and the two muons will be produced predominantly in opposite hemispheres. Since this background is too small to be measured directly from the dimuon data, it was normalised to the charm contribution to the $D^* + \mu$ sample [1], which has very similar topology, and is measured simultaneously. Other backgrounds yielding unlike-sign muon pairs include heavy quarkonium decays and Bethe-Heitler processes. In contrast to muons from semileptonic decays, muons from these sources are not directly accompanied by hadronic activity, thus giving an isolated muon signature.

Beauty production is the only source of genuine like-sign dimuon pairs. Background contributions to both like- and unlike-sign combinations include events in which either one

or both muons are fake, i.e. originate from $K \rightarrow \mu$ or $\pi \rightarrow \mu$ decays, or misidentified hadrons. Dedicated studies have shown that, for all relevant distributions of this background, the charge of the two muons is almost uncorrelated, i.e. the contributions to the like- and unlike-sign dimuon distributions are almost equal. The *difference* between the unlike- and like-sign distributions is thus essentially free from fake-muon background, without the need to simulate this background with Monte Carlo (MC) methods. Once the other background contributions are known, the difference can therefore be used to measure the beauty contribution. This in turn can be used to *measure* the fake muon background by subtracting the beauty contribution from the total like-sign sample, and mirroring it onto the unlike-sign sample.

In this analysis, the beauty signal was hence extracted from the *difference* between the like and unlike-sign samples, while the like-sign sample was used to fix the contribution from fake-muon background to the unlike-sign sample.

3 Analysis

The data used in this analysis were collected in the ZEUS detector [7] during the years 1996-97 (1998-2000), when a proton beam of 820 (920) GeV collided with an electron or positron beam of 27.5 GeV. The centre-of-mass energy was $\sqrt{s} = 300$ GeV during the period 1996-97 and $\sqrt{s} = 318$ GeV during 1998-2000. In order to present results from the combined data sets, the measurements from the 1996-97 run have been corrected to correspond to the higher centre-of-mass energy. All cross sections are therefore quoted for $\sqrt{s} = 318$ GeV. The combined data sample corresponds to a total integrated luminosity of 121 ± 2 pb⁻¹. Since one of the goals is a measurement of the total beauty cross section, no attempt is made to distinguish between deep inelastic scattering (DIS) and photoproduction events.

In order to be as inclusive as possible, the trigger selection required the presence of either a muon, a charm-meson candidate, two jets, or a DIS electron. Using this redundancy, the trigger efficiency for beauty events was about $80 \pm 5\%$.

Muons were identified by requiring the presence of a reconstructed track segment in the forward, barrel or rear inner or outer muon chambers, or by a segment or energy deposit in the backing calorimeter located in between the two sets of chambers [7]. Whenever possible, these segments or deposits were matched in space to a corresponding track in the central tracking detector [8] (CTD), from which the muon momentum measurement was obtained. In the forward region, this momentum was combined with the momentum measured in the outer muon spectrometer, if available. For very forward muons, outside of the acceptance of the CTD, the momentum information was obtained from the muon

spectrometer and the main event vertex alone. If the muons are sufficiently isolated in the calorimeter, their muonic nature was confirmed by the detection of a minimum ionising energy deposit (mip) in the main ZEUS calorimeter. This highly redundant muon selection yields an efficiency of about 80% per muon for high momentum muons.

For muons detected by one muon detector only (lower quality muons), a cut on the muon transverse momentum, $p_T^\mu > 1.5$ GeV, was applied. For muons detected by specific combinations of two or more detectors (higher quality muons) this cut was lowered to $p_T^\mu > 0.75$ GeV. No explicit cut on muon pseudorapidity (η) was made. However, additional implicit cuts on p_T and η result from the detector geometry and material distribution.

Two such muon candidates were required. In addition, the total transverse energy of the event, outside a 10° cone around the forward direction, was required to be more than 8 GeV (about twice the b quark mass, reduced by the escaping final state neutrinos). Identified DIS electrons, if any, were not included in this variable. Furthermore, some technical background cleaning cuts were applied.

Monte Carlo simulations of beauty and charm production were performed using the PYTHIA [9] and RAPGAP [10] generators. The PYTHIA simulations (for photon virtuality $Q^2 < 1$ GeV²) include the direct photon-gluon-fusion process, flavour excitation in the resolved photon and proton, and corresponding processes in which the photon acts as a hadron-like source of light partons. For $Q^2 > 1$ GeV² only the direct photon-gluon-fusion process was simulated using RAPGAP. The leading order matrix elements for all these processes are complemented by initial and final state parton showering. The detector simulation provides both real and fake muons in charm and beauty events. The light flavour background was estimated directly from the data. Charm background containing fake muons is included in the light flavour background determination, and was therefore removed from the charm MC. Backgrounds from heavy quarkonia and Bethe-Heitler processes were simulated using the HERWIG [11] and LPAIR [12] MC programs. The MC muon efficiencies were corrected on an event-by-event basis using correction factors extracted from studies of elastic J/ψ and Bethe-Heitler production in dedicated data and MC samples.

The resulting dimuon mass distributions for the low and high mass, like and unlike-sign subsamples are shown in Fig. 1. The high mass region is already strongly beauty enriched, while the low mass region exhibits a significant contribution from J/ψ production not originating from b decays. To reduce this contribution, as well as corresponding contributions from ψ' , Υ and Bethe-Heitler processes, a non-isolation cut was applied: the total energy $I_{1,2}$ deposited in a cone of $\Delta R = \sqrt{\Delta\phi^2 + \Delta\eta^2} = 1$ around each muon flight direction was calculated, excluding the other muon. The quadratic sum $I = \sqrt{I_1^2 + I_2^2}$ of the two energy deposits was required to be more than 250 MeV. For events in the J/ψ and ψ' mass peaks, where this background is largest, the cut was raised to 2 GeV.

4 Signal extraction

Figure 2 shows the muon p_T and η distribution for nonisolated unlike-sign dimuon pairs, combining the low and high mass samples. The remaining contribution from J/ψ , Bethe Heitler (BH), etc. processes was normalised such that the corresponding isolated distributions, in which these processes dominate, are reproduced. The charm contribution is small and was normalised to the charm signal in the $D^* + \mu$ sample as outlined in section 2. The total like+unlike-sign beauty contribution was extracted using the formula

$$N_{b\bar{b} \rightarrow \mu\mu} = (N_{\text{data}}^{\text{unl}} - N_{\text{data}}^{\text{like}} - (N_{\text{charm}} + N_{J/\psi} + N_{\text{BH}} + \dots)) \times \left(\frac{N_{b\bar{b}}^{\text{unl}} + N_{b\bar{b}}^{\text{like}}}{N_{b\bar{b}}^{\text{unl}} - N_{b\bar{b}}^{\text{like}}} \right)_{\text{MC}} \quad (1)$$

Corrections to this formula were applied in order to account for small (4% on average) mass-dependent asymmetries between the like and unlike sign light flavour background distributions. A total beauty contribution of about 1800 events was obtained with a purity of about 50%.

5 Total $b\bar{b}$ cross section

The low muon p_T threshold translates into sensitivity to b -quark production down to $p_T^b = 0$ (Fig. 3). In combination with the large pseudorapidity coverage, this allows the extraction of the total cross section for beauty production. In order to agree with the data, the normalisation of the PYTHIA + RAPGAP MC prediction for the beauty contribution had to be scaled up by a factor 2.06. The total cross section for $b\bar{b}$ pair production in ep collisions at HERA for $\sqrt{s} = 318$ GeV was obtained to be

$$\sigma_{\text{tot}}(ep \rightarrow b\bar{b}X) = 16.1 \pm 1.8(\text{stat.})_{-4.8}^{+5.3}(\text{syst.}) \text{ nb},$$

where the first uncertainty is statistical, and the second systematic, the sources of which are discussed below.

To investigate how much the extracted total cross section depends on details of the $b\bar{b}$ production kinematics in phase space regions which might not be covered by the measurement, an intermediate visible cross section is extracted for the maximum possible muon phase space region allowed by the preselection and the detector acceptance. Using the criterion that the muon detection efficiency should be at least about 30% per muon, this phase space was obtained to be

- $-2.2 < \eta < 2.5$ for both muons
- $p_T > 1.5$ GeV for one of the two muons

- ($p > 1.8$ GeV for $\eta < 0.6$, ($p > 2.5$ GeV or $p_T > 1.5$ GeV) for $\eta > 0.6$) and $p_T > 0.75$ GeV for the other muon.

Correcting for muon acceptance, a visible cross section for dimuon production from beauty decays in this phase space

$$\sigma_{\text{vis}}(ep \rightarrow b\bar{b}X \rightarrow \mu\mu X') = 63 \pm 7(\text{stat.})_{-18}^{+20}(\text{syst.}) \text{ pb}$$

was obtained. This cross section includes muons from direct b hadron decays, and indirect decays via intermediate charm hadrons or τ leptons. The muons can either originate from the same b quark, or from different quarks of the $b\bar{b}$ pair. Muonic decays of kaons, pions or other light hadrons are not included. An event containing more than two muons was counted only once.

Dividing this cross section by the probability of a $b\bar{b}$ pair to yield a muon pair in this kinematic range, the total cross section already quoted above can again be obtained. This probability (0.38% on average) is quite small. However, it is almost entirely dominated by quantities measured with good precision at e^+e^- colliders. The effective branching fraction of a $b\bar{b}$ pair into at least two muons is 6.3% [9, 13]. Both the b fragmentation functions and the b hadron $\rightarrow \mu X$ decay spectra are well measured [13] and yield an average acceptance for the visible range of 6%. Furthermore, the value of this acceptance varies by only a factor 3 (about 3 to 9%) in 90% of the $b\bar{b}$ phase space, delimited by $0 < p_{Tb}^{\text{max}} < 10$ GeV or $|\zeta_b|^{\text{min}} < 2$. Here p_{Tb}^{max} denotes the maximum p_T of the two b quarks after parton showering, and $|\zeta_b|^{\text{min}}$ the minimum of the modulus of the rapidity (not pseudorapidity) of the two quarks. At larger p_{Tb} the acceptance rises, but the fraction of events is small. In rapidity, only 10% of the total beauty contribution in the region $\zeta_b^{\text{min}} > 2$ remains unmeasured. This uniformity of acceptance means that the dependence on details of the simulation of the $b\bar{b}$ topology is rather weak, and that the extrapolation to unmeasured regions is small.

It was checked that the b -quark spectra from PYTHIA and RAPGAP agree well with the corresponding spectra from the NLO predictions described below. Nevertheless, the systematic uncertainty associated to this source was estimated from drastic changes such as using the PYTHIA direct contribution only, or doubling the nondirect contributions for the acceptance calculation. This changed the measured cross sections by only about 10%.

The biggest systematic uncertainty arises from the muon efficiency correction. Other uncertainties include the variation of branching ratios and decay spectra, the $B^0 - \bar{B}^0$ mixing parameter, and an adequate variation of the charm, J/ψ , and Bethe-Heitler backgrounds.

Uncertainties due to calorimetry, tracking, and luminosity measurement were found to be almost negligible compared to the other errors.

6 Differential cross sections and $b\bar{b}$ correlations

The same method was used to derive differential cross sections. To simplify the measurements, true muon phase space was restricted to $p_T^\mu > 1.5$ GeV and $-2.2 < \eta^\mu < 2.5$ for both muons. The $p_T^\mu > 1.5$ GeV cut was explicitly required also at reconstruction level. This retained about 2/3 of the originally selected sample. The signal-extraction procedure was the same as for the inclusive visible cross section, except that it is now applied bin-by-bin. Bin-dependent systematic uncertainties were calculated wherever possible. The resulting cross sections for the differential p_T^μ and η^μ spectra are shown in Figs. 4 and 5. Very good agreement is observed with the PYTHIA+RAPGAP predictions scaled by a factor 1.95. This factor is essentially the same as that for the slightly looser inclusive selection. Apart from the normalisation, the leading order + parton shower (LO+PS) approach yields a good description of the corresponding physics processes within the entire accessible phase space.

To have a more detailed look at the correlations between the two b -quarks, the reconstructed dimuon mass range was restricted to $m_{\text{inv}}^{\mu\mu} > 3.25$ GeV. This reduced the contribution of dimuons from the same quark to an almost negligible level. The corresponding data distribution for $\Delta\phi$ between the two muons is shown in Fig. 6. Consequently, at true level, muons were now required to originate from different b -quarks. This results in the differential cross section shown in Fig. 7. The distribution is again well described by the LO+PS MC within the large errors resulting from the subtraction method.

7 Comparison to NLO predictions and other measurements

The total cross section predicted by next-to-leading order (NLO) QCD calculations were obtained in the massive approach by adding the predictions from FMNR [14] and HVQDIS [15] for $Q^2 <, > 1$ GeV², respectively. The default renormalisation and factorisation scales of these calculations are varied by a factor 2, and the b -quark mass was varied between 4.5 and 5 GeV. The CTEQ5M/CTEQ5F4 structure functions were used. The resulting cross section for $\sqrt{s} = 318$ GeV

$$\sigma_{\text{tot}}^{\text{NLO}}(ep \rightarrow b\bar{b}X) = 6.8_{-1.7}^{+3.0} \text{ nb}$$

is a factor 2.4 lower than the measured value, although still compatible within the large uncertainties (about two standard deviations).

Figure 8 shows a comparison of this cross section to the slightly less inclusive cross sections from the $D^* + \mu$ final state obtained by ZEUS in earlier measurements [1]. These

measurements, as well as similar measurements by H1 [2] show the same trend to be larger than the corresponding QCD predictions.

8 Conclusions

The total cross section for beauty production in ep collisions at HERA has been measured using an analysis technique based on the detection of two muons, mainly from semileptonic beauty decay. The resulting visible cross section exceeds leading-order plus parton-shower MC expectations. The almost complete phase space coverage and only weak dependence on details of the $b\bar{b}$ event topology allows a reliable extraction of the total beauty production cross section, with small extrapolation, and a direct comparison to NLO QCD predictions. The trend that QCD calculations near kinematic threshold tend to underestimate the beauty cross section at HERA, also observed in other measurements [1, 2], is intriguing, although the predictions are not incompatible with the ZEUS measurements. Differential cross sections in p_T^μ , η^μ , and $\Delta\phi^{\mu\mu}$ were also obtained, and found in very good agreement with the shapes predicted by Monte Carlo models incorporating leading order matrix elements followed by parton showers.

References

- [1] ZEUS Coll. Abstract 5-0342, 11-0343, International Conference on High Energy Physics, Beijing, China, August 16-22, 2004;
ZEUS Coll. Abstract 784, International Conference on High Energy Physics, Amsterdam, The Netherlands, July 24-31, 2002.
- [2] H1 Coll., A. Aktas et al., hep-ex/0503038 (2005).
- [3] H1 Coll., C. Adloff et al., Phys. Lett. **B 467**, 156 (1999);
ZEUS Coll., J. Breitweg et al., Eur. Phys. J. **C 18**, 625 (2001).
- [4] ZEUS Coll., S. Chekanov et al., Phys. Rev. **D 70**, 012008 (2004);
ZEUS Coll., S. Chekanov et al., Phys. Lett. **B 599**, 173 (2004);
H1 Coll., A. Aktas et al., hep-ex/0502010 (2005).
- [5] H1 Coll., A. Aktas et al., Eur. Phys. J. **C40**, 349 (2005).
- [6] H1 Coll. H1prelim-04-173, presented at ICHEP2004, summer 2004;
H1 Coll. H1prelim-05-076, presented at DIS2005, spring 2005.
- [7] ZEUS Coll., U. Holm (ed.), *The ZEUS Detector*. Status Report (unpublished), DESY (1993), available on <http://www-zeus.desy.de/bluebook/bluebook.html>.
- [8] N. Harnew et al., Nucl. Inst. Meth. **A 279**, 290 (1989);
B. Foster et al., Nucl. Phys. Proc. Suppl. **B 32**, 181 (1993);
B. Foster et al., Nucl. Inst. Meth. **A 338**, 254 (1994).
- [9] T. Sjöstrand, Comp. Phys. Comm. **82**, 74 (1994).
- [10] H. Jung, Comp. Phys. Comm. **86**, 147 (1995).
- [11] G. Marchesini et al., Comp. Phys. Comm. **67**, 465 (1992).
- [12] S.P. Baranov et al., *Proc. Workshop on Physics at HERA*, W. Buchmüller and G. Ingelman (eds.), Vol. 3, p. 1478. DESY, Hamburg, Germany (1991).
- [13] Particle Data Group, S. Eidelman et al., Phys. Lett. **B 592**, 1 (2004).
- [14] S. Frixione, P. Nason and G. Ridolfi, Nucl. Phys. **B 454**, 3 (1995).
- [15] B.W. Harris and J. Smith, Nucl. Phys. **B452**, 109 (1995);
B.W. Harris and J. Smith, Phys. Lett. **B 353**, 535 (1995). Erratum-ibid **B 359** (1995) 423.

ZEUS

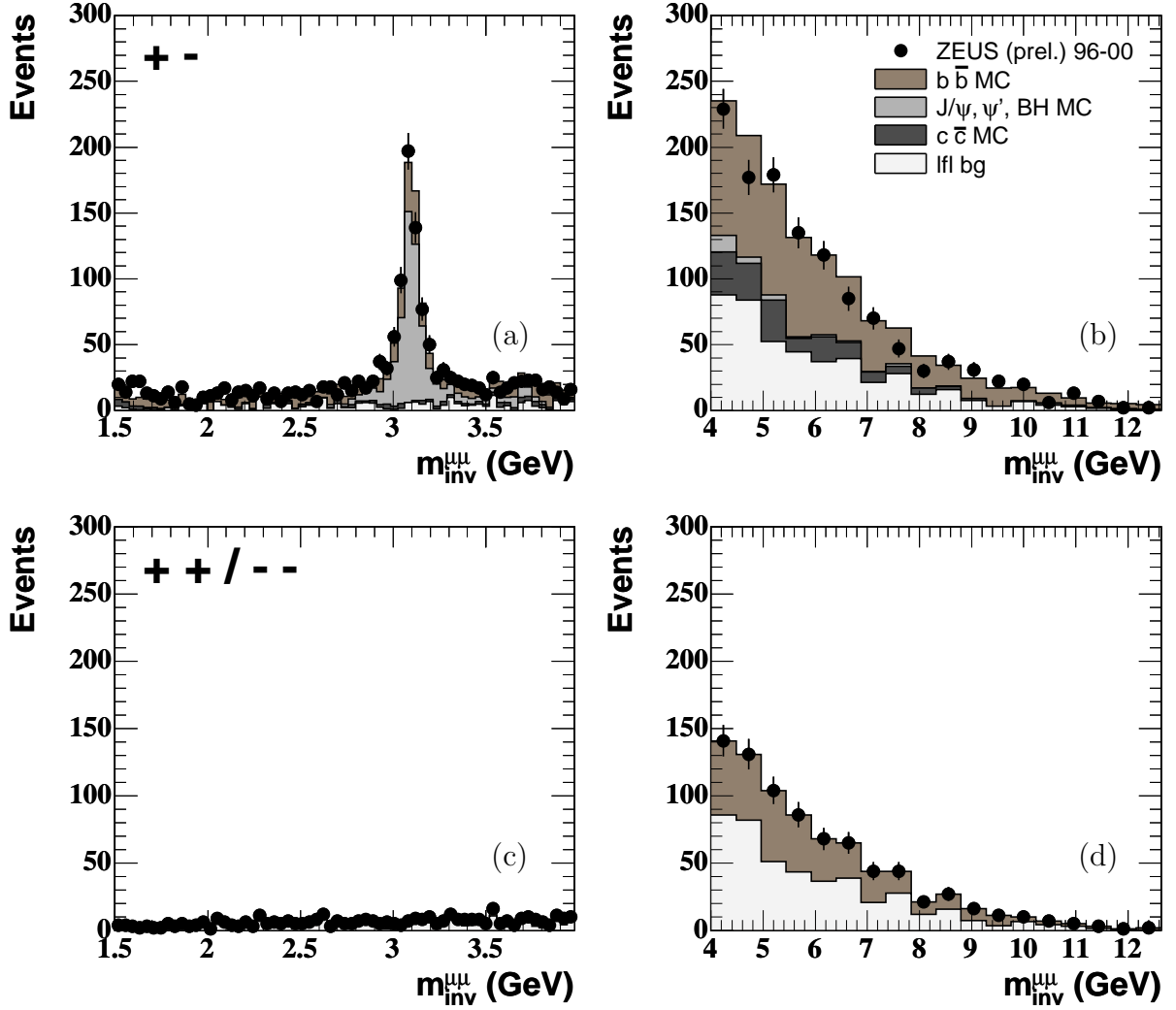


Figure 1: *Dimuon mass distributions of unlike sign dimuon pairs in the (a) low mass and (b) high mass subsamples, as well as like sign dimuon pairs in the (c) low and (d) high mass subsamples. The breakdown into the expected contributions from different processes is also shown.*

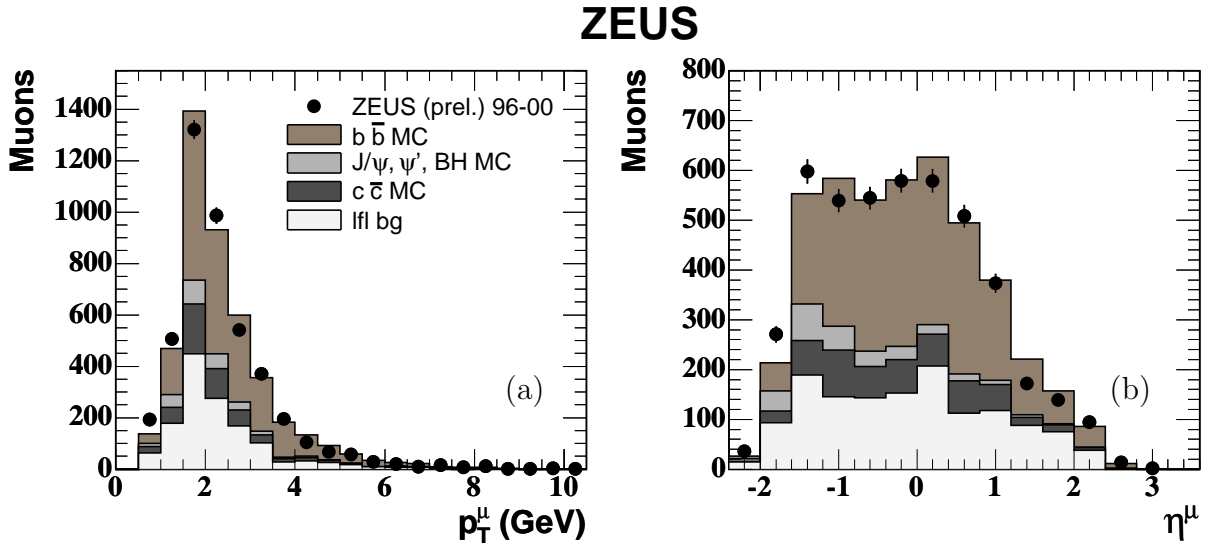


Figure 2: Muon (a) transverse momentum and (b) pseudorapidity distribution from both high and low mass dimuon pairs in the nonisolated unlike sign sample. Two muons are entered for each event. The breakdown into the expected contributions from different processes is also shown.

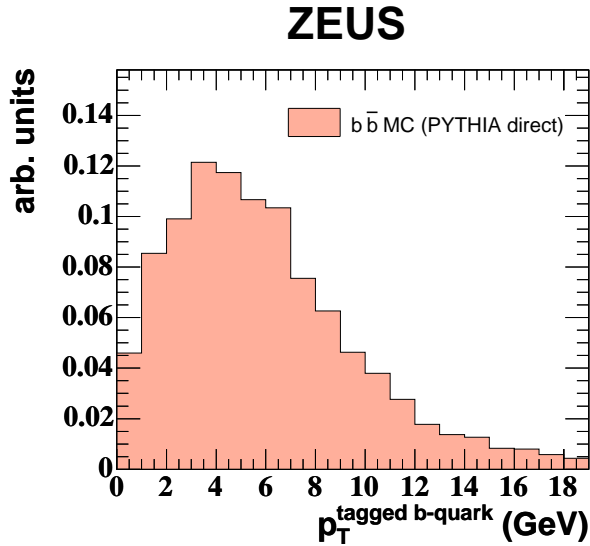


Figure 3: Example of b quark transverse momentum distribution for quarks tagged by reconstructed muons in dimuon events, from PYTHIA direct processes. The tagging method is sensitive to b quarks “at rest”, i.e. with vanishing transverse momentum.

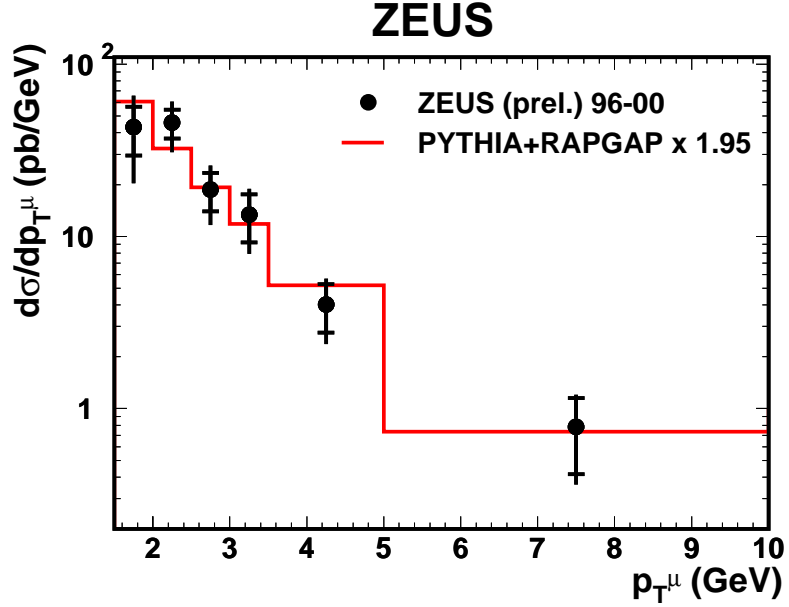


Figure 4: Cross-section $d\sigma/dp_T^\mu$ for muons from b decays in dimuon events with $p_T^\mu > 1.5$ GeV and $-2.2 < \eta^\mu < 2.5$ for both muons. Two muons contribute for each event. The data (solid dots) are compared to the scaled sum of the predictions by the LO+PS generators PYTHIA and RAPGAP (histogram).

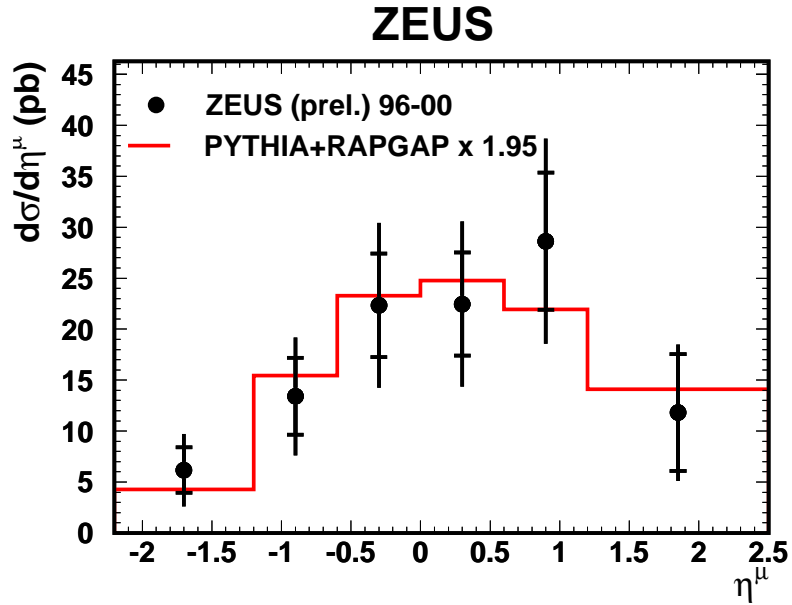


Figure 5: Cross-section $d\sigma/d\eta^\mu$ for muons from b decays in dimuon events with $p_T^\mu > 1.5$ GeV and $-2.2 < \eta^\mu < 2.5$ for both muons. Two muons contribute for each event. The data (solid dots) are compared to the scaled sum of the predictions by the LO+PS generators PYTHIA and RAPGAP (histogram).

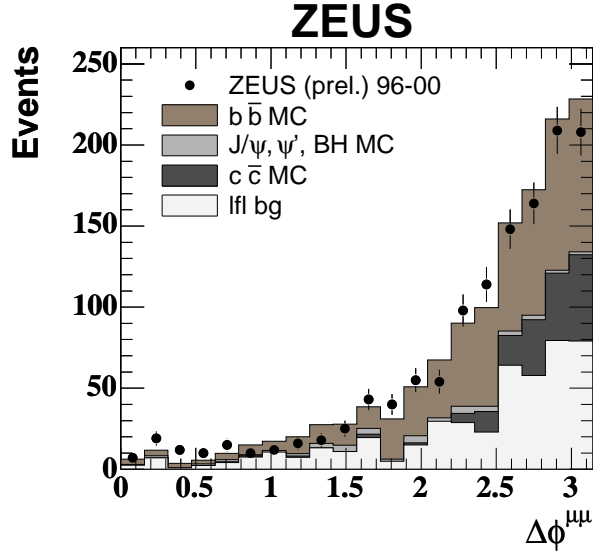


Figure 6: Distribution of the azimuthal distance $\Delta\phi$ between the two muons in dimuon events with $p_T^\mu > 1.5\text{GeV}$ and $-2.2 < \eta^\mu < 2.5$ for both muons, and $m^{\mu\mu} > 3.25\text{ GeV}$. The breakdown into the expected contributions from different processes is also shown.

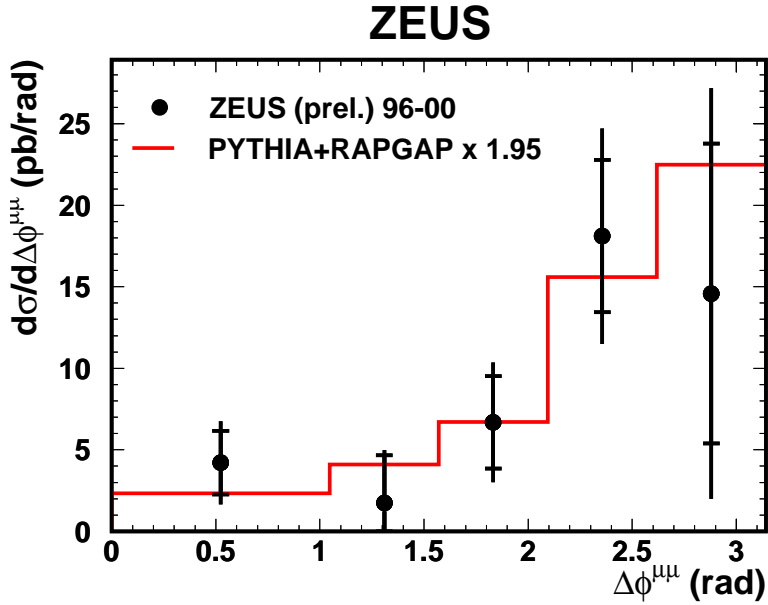


Figure 7: Cross-section $d\sigma/d\Delta\phi^{\mu\mu}$ for dimuon events from $b\bar{b}$ decays in which each muon originates from a different $b(\bar{b})$ quark, with $p_T^\mu > 1.5\text{GeV}$ and $-2.2 < \eta^\mu < 2.5$ for both muons. The data (solid dots) are compared to the scaled sum of the predictions by the LO+PS generators PYTHIA and RAPGAP (histogram).

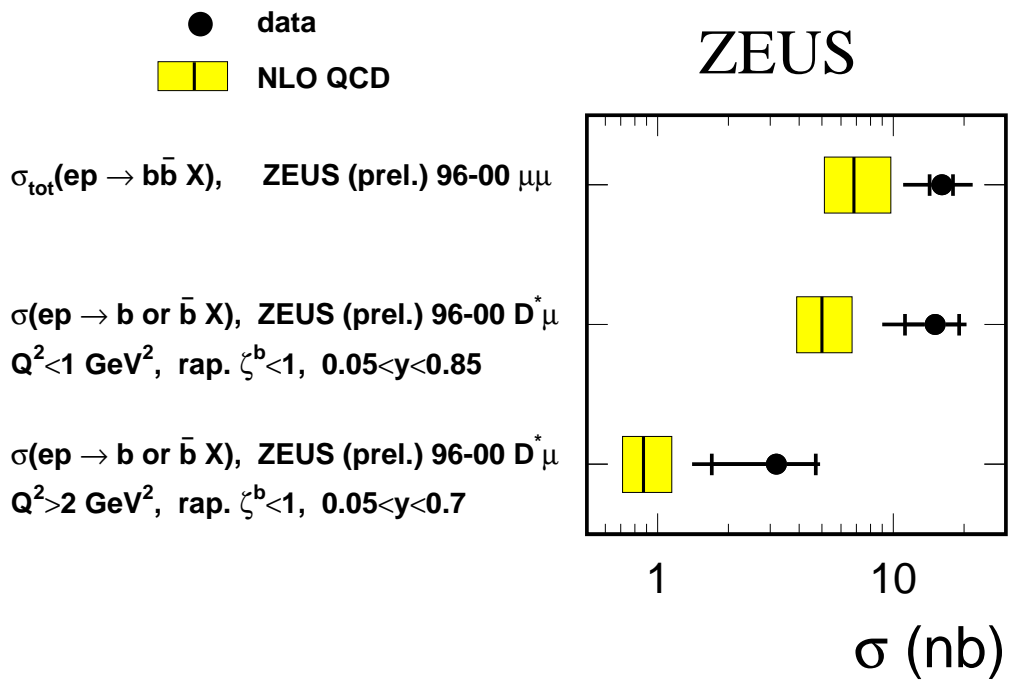


Figure 8: Comparison of measured cross sections to NLO predictions. The $\text{b}\bar{\text{b}}$ cross section from this analysis is shown at the top. For comparison, related b or $\bar{\text{b}}$ cross sections obtained in the ZEUS $D^* \mu$ analysis for the photoproduction regime (middle line) and DIS (lower line), are also shown.